HHS Public Access

Author manuscript

Cancer Discov. Author manuscript; available in PMC 2016 July 01.

Published in final edited form as:

Cancer Discov. 2016 January ; 6(1): 96–107. doi:10.1158/2159-8290.CD-15-1056.

The ALK/ROS1 inhibitor PF-06463922 overcomes primary resistance to crizotinib in ALK-driven neuroblastoma

Nicole R. Infarinato[1], **Jin H. Park**[2,3], **Kateryna Krytska**[1], **Hannah T. Ryles**[1], **Renata Sano**[1], **Katherine M. Szigety**[2,3], **Yimei Li**[1,4], **Helen Y. Zou**[6], **Nathan V. Lee**[6], **Tod Smeal**[6], **Mark A. Lemmon**[2,3,7], and **Yael P. Mossé**[1,5,*]

[1]Division of Oncology and Center for Childhood Cancer Research, The Children's Hospital of Philadelphia, Philadelphia, PA, 19104, USA

[2]Graduate Group in Biochemistry and Molecular Biophysics, Perelman School of Medicine, University of Pennsylvania, Philadelphia, PA, 19104 USA

[3]Department of Biochemistry and Biophysics, Perelman School of Medicine, University of Pennsylvania, Philadelphia, PA, 19104 USA

[4]Department of Biostatistics & Epidemiology, Perelman School of Medicine, University of Pennsylvania, Philadelphia, PA, 19104 USA

[5]Department of Pediatrics, Perelman School of Medicine, University of Pennsylvania, Philadelphia, PA, 19104 USA

[6]Oncology Research Unit, Pfizer Worldwide Research and Development, San Diego, CA, 92121, USA

Abstract

[*]Corresponding Author: Yael P. Mossé, M.D., Children's Hospital of Philadelphia, Division of Oncology, 3501 Civic Center Boulevard, CTRB 3056, Philadelphia, PA 19104, Tel: 215-590-0965, Fax: 267-426-0685, mosse@chop.edu.

[7]Present address: Department of Pharmacology and Cancer Biology Institute, Yale University, New Haven, CT 06520, USA

N. R. Infarinato and J.H. Park contributed equally to this work

M. A. Lemmon and Y. P. Mossé jointly directed this work.

Conflict of interest disclosure statement: No conflicts of interest disclosed for NRF, JHP, KK, HTR, RS, KS, MAL and YPM. HYZ, NVL and TS are employees at Pfizer, Inc.

Disclosure of Potential Conflicts of Interest

Helen Y. Zou, Nathan V. Lee, and Tod Smeal are employees and shareholders of Pfizer, Inc. Yaël Mossé is an inventor on a patent filed by the Children's Hospital of Philadelphia (WO/2009/103061 or PCT/US2009/034288: Methods and Compositions for Identifying, Diagnosing, and Treating Neuroblastoma).

Note:

Supplementary data for this article are available at Cancer Discovery Online (http://cancerdiscovery.aacrjournals.org/).

Authors' Contributions

Conception and design: N.R. Infarinato, J.H. Park, M.A. Lemmon, and Y.P. Mossé

Development of methodology: N.R. Infarinato, J.H. Park, K. Krytska, M.A. Lemmon, and Y.P. Mossé

Acquisition of data (provided animals, acquired and managed patients, provided facilities, etc.): N.R. Infarinato, J.H. Park, K. Krytska, H.T. Ryles, R. Sano, H.Y. Zou, N.V. Lee, T. Smeal, M.A. Lemmon, and Y.P. Mossé

Analysis and interpretation of data (e.g., statistical analysis, biostatistics, computational analysis): N.R. Infarinato, J.H. Park, K. Krytska, Y. Li, M.A. Lemmon, and Y.P. Mossé

Writing, review, and/or revision of the manuscript: N.R. Infarinato, J.H. Park, K. Krytska, H.T. Ryles, R. Sano, Y. Li, H.Y. Zou, N.V. Lee, T. Smeal, M.A. Lemmon, and Y.P. Mossé

Administrative, technical, or material support (i.e., reporting or organizing data, constructing databases): N.R. Infarinato, J.H. Park, H.Y. Zou, N.V. Lee and T. Smeal

Study supervision: Y.P Mossé and M.A. Lemmon

Neuroblastomas (NBs) harboring activating point mutations in Anaplastic Lymphoma Kinase (ALK) are differentially sensitive to the ALK inhibitor crizotinib, with certain mutations conferring intrinsic crizotinib resistance. To overcome this clinical obstacle, our goal was to identify inhibitors with improved potency that can target intractable ALK variants such as F1174L. We find that PF-06463922 has high potency across ALK variants, and inhibits ALK more effectively than crizotinib *in vitro*. Most importantly, PF-06463922 induces complete tumor regression in both crizotinib-resistant and sensitive xenograft mouse models of NB, as well as in PDXs harboring the crizotinib-resistant F1174L or F1245C mutations. These studies demonstrate that PF-06463922 has the potential to overcome crizotinib resistance, and exerts unprecedented activity as a single targeted agent against F1174L and F1245C *ALK*-mutated xenograft tumors, while also inducing responses in a R1275Q xenograft model. Taken together, these results provide the rationale to move PF-06463922 into clinical trials for treatment of patients with *ALK*-mutated NB.

Keywords

neuroblastoma; kinase inhibitor; resistance; crizotinib

INTRODUCTION

Neuroblastoma is a devastating pediatric cancer of the autonomic nervous system accounting for 12% of childhood cancer deaths (1). Despite major enhancements in treatment approaches, including integration of immunotherapeutic strategies (2), the cure rate for patients with high-risk neuroblastoma remains unsatisfactory. Several recent findings have positioned the Anaplastic Lymphoma Kinase (ALK) receptor tyrosine kinase as the only tractable oncogene product for targeted therapy in neuroblastoma. Germline and somatic aberrations in the gene encoding ALK are implicated in approximately 8% of all neuroblastomas (3–6). Within the high-risk subset of neuroblastoma patients, the overall frequency of *ALK* aberration at diagnosis is 14% (10% point mutations, 4% amplification) and correlates with inferior outcome (7). Additional *ALK* mutations at relapse have also been reported (8, 9). The activating mutations are found at several sites in the tyrosine kinase domain of full-length ALK (7), including three hot spots (R1275, F1174, and F1245). These findings motivated a Phase 1 trial of the ATP-competitive ALK/Met/ROS1 inhibitor crizotinib (PF-02341066) in children with refractory neuroblastoma or other malignancies driven by *ALK* rearrangements such as anaplastic large cell lymphoma (ALCL) and inflammatory myofibroblastic tumors (IMTs) (10). Results from this trial underscored the importance of *ALK* across histologically diverse tumors, but recorded less frequent responses in neuroblastoma than in *ALK* rearranged tumors – highlighting likely differences between therapeutic targeting of full-length ALK in neuroblastoma and of cytoplasmic ALK fusion proteins in ALCL, IMTs, and lung cancer. Parallel preclinical work has further revealed differential sensitivity to crizotinib for the most common ALK variants observed in neuroblastoma (11–13), with F1174L-mutated cells being resistant when compared with those expressing R1275Q-mutated ALK. Despite real-time integration of these findings in the clinic, and a recommended phase 2 dose of crizotinib in pediatric patients that is nearly twice the adult maximum tolerated dose (10), these studies emphasize the need to identify an

optimal inhibitor for direct ALK kinase inhibition in neuroblastoma in order to maximize clinical benefit.

Our previous studies indicated that the relative crizotinib sensitivities of ALK variants may simply reflect their ATP-binding affinities, with reduced $K_{M,ATP}$ (higher ATP-binding affinity) predicting crizotinib resistance for F1174L-mutated ALK, for example (11). We explored two strategies to overcome this problem. In the first, we tested a series of second-generation ALK kinase inhibitors, anticipating that their structural differences might allow some to show selective (or improved) inhibition of F1174L-mutated ALK – as has been suggested for other ALK variants (14). As we failed to find any inhibitors with these characteristics, our second approach was to investigate the impact of increasing drug-binding affinity to all ALK variants – made possible by using the highly potent ALK/ROS1 inhibitor PF-06463922 (15, 16). We hypothesized that a drug with substantially increased ALK-binding affinity might be capable of inhibiting all ALK variants at readily achievable drug concentrations, and that this feature might negate the effects of primary resistance mutations. We show here that PF-06463922 has substantially greater potency than crizotinib as an ALK inhibitor *in vitro* – across all neuroblastoma mutations tested. Most importantly, PF-06463922 also showed excellent activity against full-length oncogenic ALK variants in pre-clinical models of ALK-driven neuroblastoma where crizotinib fails. Through biochemical, cell-based, xenograft and patient-derived xenograft (PDX) studies, we demonstrate that PF-06463922 has unprecedented activity as a single agent against *ALK*-mutants, including those with primary crizotinib resistance – thus positioning PF-06463922 as the lead ALK inhibitor for clinical development in ALK-driven neuroblastoma.

RESULTS

In our earlier studies, we were able to recapitulate the differential crizotinib sensitivity of F1174L and R1275Q ALK variants *in vitro*, using kinase assays (11). We also showed that the transforming ability of ALK variants correlates most closely with *in vitro* k_{cat} values for the unphosphorylated kinase domain of the receptor (7) – implying that activation of this species is key for oncogenesis. Unfortunately, a preliminary screen through a series of second-generation ALK inhibitors failed to identify any that differed significantly from crizotinib in their relative ability to inhibit R1275Q, F1174L, and F1245C variants of the unphosphorylated ALK tyrosine kinase domain (ALK-TKD) *in vitro*. The ALK/ROS1 inhibitor PF-06463922 stood out starkly in these assays, however, by yielding uniquely low IC_{50} values. As previously pointed out (16), PF-06463922 is more potent against wild-type ALK than crizotinib, alectinib, or ceritinib by 4-fold or more when K_i values are compared. In our *in vitro* experiments, PF-06463922 gave IC_{50} values for inhibition of F1174L and F1245C-mutated ALK that were significantly lower than seen with crizotinib even for the crizotinib-sensitive R1275Q variant (Fig. 1A and B)). Indeed, measured IC_{50} values for PF-06463922 were ~5 fold lower than for crizotinib for all variants, and were actually limited in this assay by the concentration of kinase protein required to measure activity of unphosphorylated ALK-TKD (50 nM). Estimated K_i values from our data using the equations of Cha (17) are less than 0.2 nM for inhibition of mutated ALK-TKD by PF-06463922, compared with 6–10 nM for crizotinib inhibition – K_i values consistent with previous reports using different methods and different sets of mutations (15, 16). Thus,

PF-06463922 is a very potent inhibitor for multiple mutated full-length ALK variants seen in neuroblastoma, as also reported for acquired resistance mutations seen in cytoplasmic ALK fusion proteins in lung cancer and elsewhere (15, 16, 18). We hypothesized that this significantly increased potency and/or affinity of PF-06463922 compared with other ALK inhibitors in development might be sufficient to negate the consequences of differential sensitivity of ALK variants to kinase inhibitors.

PF-06463922 induces complete tumor regression in patient-derived and cell line-derived xenografts with and without primary resistance to crizotinib

The data in Figure 1 suggest that F1245C-mutated ALK should resemble F1174L-mutated ALK in its primary resistance to crizotinib – consistent with limited clinical data (10) – but that tumors driven by all three hot spot ALK variants should respond to PF-06463922. To test these hypotheses, we compared *in vivo* efficacies of PF-06463922 and crizotinib in crizotinib-naive patient-derived xenografts (PDXs) harboring F1174L or F1245C *ALK* mutations (COG-N-453x and Felix-PDX respectively), as well as cell line-derived xenografts utilizing SH-SY5Y cells (F1174L) or NB-1643 cells (R1275Q). Tumor-bearing animals were treated by oral gavage either with 5 mg/kg PF-06463922 twice daily (BID) or 100 mg/kg crizotinib once daily (QD). Two of the models (Felix-PDX and SH-SY5Y) were treated for 6-weeks, while the new COG-N-453x PDX and NB-1643, both slightly more sensitive to crizotinib, were treated for longer (8.1 and 8.9 weeks, respectively). Crizotinib and PF-06463922 at these doses were both well-tolerated (Fig. S1A–D). As expected, crizotinib alone at 100 mg/kg/day demonstrated limited inhibition of tumor growth in these models. Crizotinib delayed growth in both PDXs (Figs. 2A and B), such that tumor volume at any given time was ~30% of that seen in vehicle-treated mice. The SH-SY5Y (F1174L) xenograft showed no response to crizotinib (Fig. 2C). By contrast, the NB-1643 (R1275Q) xenograft showed an initial response with essentially no tumor growth for 3.5 weeks when treated with crizotinib – as previously described (11) – although significant tumor growth was seen after 4 weeks (Fig. 2D).

Contrasting with these limited – or transient – responses to 100 mg/kg/day crizotinib, treatment with 10 mg/kg/day PF-06463922 (5 mg/kg BID) resulted in rapid (within 2–3 weeks) and sustained complete tumor regression for the duration of treatment in all xenografts (red curves in Fig. 2, and Table 1A). After PF-06463922 treatment was stopped, animals were further monitored for tumor progression by observation and palpation. Mice that had been treated with 10 mg/kg/day PF-06463922 remained in complete remission with no discernible tumor growth for a further 4.8 weeks (COG-N-453x), 7.1 weeks (Felix-PDX), 5 weeks (SH-SY5Y) and 4 weeks (NB-1643), as shown in Fig. S2A–D. Thus, xenografts harboring the *de novo* crizotinib-resistant ALK F1174L mutation exhibited unprecedented anti-tumor responses to single agent ALK inhibition therapy with PF-06463922, as did a PDX harboring the F1245C mutation.

Given these rapid and complete responses to 10 mg/kg/day PF-06463922 in Fig. 2, we also evaluated a lower dose of 3 mg/kg/day (1.5 mg/kg BID) in both the Felix-PDX (F1245C) PDX and SH-SY5Y (F1174L) xenograft. As shown in Fig. S3A–B and Table 1B, this lower PF-06463922 dose was still substantially more effective than a 33-fold higher dose of

crizotinib. In the SH-SY5Y xenograft (Fig. S3B), 3 mg/kg/day PF-06463922 induced complete regression within 6 weeks of treatment (compared with 2–3 weeks for 10 mg/kg/day PF-06463922). The lower dose of PF-06463922 caused significant growth delay in Felix-PDX (Fig. S3A), with tumors remaining palpable throughout treatment and showing little further growth after approximately 4 weeks. PF-06463922 at both dosing levels significantly prolonged event-free survival (EFS) relative to control and crizotinib arms in SH-SY5Y and Felix xenografts (Fig. S3, and Table 1B).

PF-06463922 efficiently inhibits ALK phosphorylation *in vivo*

To compare the effects of the two ALK inhibitors on ALK activity, we used immunoblotting to analyze pALK levels in tumor lysates from NB1643 xenografts treated with vehicle, PF-06463922, or crizotinib. Tumors were harvested after 3 days of drug treatment, 1 h after the last dose. As shown in Fig. 3, pALK was essentially undetectable in tumors from the PF-06463922-treated mice, whereas tumors from crizotinib-treated mice retained significant ALK phosphorylation. Interestingly, crizotinib appeared to suppress ALK phosphorylation at Y1278 (Fig. 3A), in the activation loop of the TKD, more completely than Y1604 (Fig. 3B) – which lies in the regulatory C-terminal tail of the receptor. By contrast, PF-06463922 at 10 mg/kg/day almost completely suppressed phosphorylation at both sites. Thus, consistent with its more potent inhibition of *in vivo* growth of ALK-dependent tumors, PF-06463922 appears to suppress ALK phosphorylation more effectively than crizotinib – even at a 10-fold lower daily dose.

PF-06463922 inhibits growth of *ALK*-mutated neuroblastoma cell lines at ~20–125 fold lower concentrations than crizotinib

To compare PF-06463922 and crizotinib over a broader range of ALK-driven tumors, we assessed their abilities to inhibit growth of a range of cell-lines *in vitro*, employing a CellTiter-Glo luminescent cell viability assay. As shown in Fig. 4 and Table S1, IC_{50} values measured for PF-06463922 in neuroblastoma cell-lines dependent on R1275Q-mutated ALK were 51-fold (NB-1643) and 19-fold (LAN-5) lower than those measured for crizotinib (Fig. 4A and B) – which themselves were ~310 nM. Importantly, IC_{50} values for PF-06463922 inhibition of cell-lines driven by the ALK-resistant F1174L ALK variant were also much lower – falling in the range of 12.7 nM to 26.6 nM, which is ~30-fold lower than measured for crizotinib (Fig. 4C–F and Table S1). A similar difference was also seen for Felix cells, driven by the F1245C variant (Fig. 4G). Whereas a small (~3-fold) difference in IC_{50} appeared to be sufficient to explain the relative crizotinib resistance of tumors and cell-lines driven by F1174L-mutated ALK in neuroblastoma compared with those driven by R1275Q (11), the overall higher potency of PF-06463922 appears to render such differences irrelevant – so that both tumor cell-lines (Fig. 4) and xenografts (Fig. 2) driven by the F1174L variant are sensitive to PF-06463922. The same appears to be true for the F1245C variant. Similar results were seen for NB-1 cells, driven by amplified wild-type ALK – with IC_{50} values of 256 nM and 5.2 nM for crizotinib and PF-06463922 respectively (Fig. 4H).

Three other interesting observations emerge from this study. First, the difference in IC_{50} values for crizotinib and PF-06463922 is even greater (>100-fold) for the NCI-H3122 lung cancer cell-line driven by the EML4-ALK fusion (Fig. 4I and Table S1), suggesting that the

presence of the TKD in the intact receptor might slightly limit the potency of PF-06463922. Second, in agreement with previous studies (16), PF-06463922 is less toxic than crizotinib in cell-lines that are not dependent on ALK for growth (Fig. 4J and K) – consistent with its high selectivity (15). Third, PF-06463922 treatment did not cause complete growth inhibition in cell lines with R1275Q, F1174L, or F1245C mutations, whereas crizotinib does. One possible explanation for the plateau in PF-06463922 activity might be its higher specificity for ALK and ROS1 (15), with limited off-target effects. The additional diminution of cell viability with crizotinib might arise from its ability to inhibit other kinases including c-Met, and RON (19) which could possibly contribute to tumor cell growth. A similar phenomenon is seen in several lung cancer cell-lines driven by ALK fusion proteins harboring resistance mutations (16).

Comparison of effects on ALK phosphorylation in cell lines

In an effort to correlate the lower IC_{50} values seen for PF-06463922 in cell viability studies in Fig. 4 with ALK inhibition, we also compared effects of PF-06463922 and crizotinib on ALK phosphorylation in neuroblastoma cell-lines harboring different ALK variants (Figs. 5A and B). Both inhibitors substantially diminish ALK phosphorylation at Y1278 (in the activation loop of the kinase). Consistent with the lower IC_{50} values observed for PF-06463922 for effects on viability of R1275Q-expressing NB-1643 cells, the pALK signal is almost completely abolished at 100 nM PF-06463922, although some signal remains with the equivalent concentration of crizotinib (Fig. 5A). Similarly, at any given concentration of drug, PF-06463922 treatment appears to promote greater diminution of the pALK signal than crizotinib in F1174L-expressing SH-SY5Y cells (Fig. 5B). It is interesting, however, that the difference between PF-06463922 and crizotinib is more stark for the EML4-ALK driven NCI-H3122 lung cancer cell-line (Fig. 5C) – as also seen in the cell viability studies. Indeed, across the board, as listed in Table S1, IC_{50} values for PF-06463922 in cell viability studies are approximately 10-fold higher for the ALK-dependent neuroblastoma cell-lines (10–30 nM) than for the *ALK*-translocated lung cancer line (IC_{50} = 2.8 nM). Zou et al. (16) recently reported PF-06463922 IC_{50} values in the 2–3 nM range for cells driven by EML4-ALK fusions, but higher values (similar to those seen for neuroblastoma cells) in the cells expressing mutated EML4-ALK. In all cases, however, the superior potency of PF-06463922 is such that the IC_{50} values are sufficient to predict clinical efficacy.

Inhibition of NIH 3T3 cell transformation by mutated ALK

To compare the effects of the two ALK inhibitors on mutated ALK variants all in a common cell background, we also analyzed their ability to inhibit ALK-mediated transformation of NIH 3T3 cells in focus assays as described (7). As shown in Fig. 6A–C, PF-06463922 was substantially more effective than crizotinib at blocking transformation/focus formation induced by ALK with any of the three hot spot mutations. IC_{50} values were consistently 5–10 fold lower for PF-06463922 than for crizotinib, consistent with experiments in all other *in vitro* and *in vivo* contexts described here. It is interesting, however, that NIH 3T3 cells expressing the R1275Q variant were significantly more sensitive to both drugs than cells expressing F1174L or F1245C mutated ALK. Indeed, the IC_{50} values for inhibition of focus formation in R1275Q-expressing cells (Fig. 6A) were lower than in F1174L-expressing cells (Fig. 6B) by 3.1-fold and 4.3 fold for crizotinib and PF-06463922 respectively. These

numbers are greater than can be explained based on *in vitro* IC_{50} or K_i values for the two variants (Fig. 1) or on their relative $K_{M,ATP}$ values (11). In turn, these data suggest that there is an additional characteristic of R1275Q-mutated ALK that may render tumors driven by it more sensitive to ALK inhibitors. Possibilities would include altered trafficking rates and/or signaling specificity, for example (20). A key finding, however, is that the IC_{50} values measured with PF-06463922 for all variants are lower than that measured for crizotinib with the crizotinib-sensitive R1275Q variant.

DISCUSSION

Although our work, and that of others, has positioned ALK as the first tractable oncogene for targeted therapy in neuroblastoma, it is now clear that not all *ALK* mutations impart oncogenic dependency (7, 12). Moreover, susceptibility of ALK-driven tumors and cell-lines to crizotinib differs according to the underlying mutation (11, 21), with mutations at two of the three hotspots (F1174 and F1245) apparently causing primary resistance to ALK kinase inhibition with crizotinib (7, 11). Consistent with this, whereas marked anti-tumor activity was observed in the COG phase 1 trial of crizotinib in pediatric patients with diseases caused by *ALK* translocations, far fewer objective responses were seen in patients with *ALK*-mutated neuroblastoma (10). We therefore sought alternative ALK inhibition strategies to overcome this intrinsic resistance. Here, we report that the superior potency of PF-06463922 as an ALK kinase inhibitor delivers impressive activity across a range of *in vitro* and *in vivo* preclinical studies in which significant resistance is detected with all other inhibitors that we have tested, including crizotinib (11). Effective doses of PF-06463922 were 10–30 fold lower than those required for crizotinib in these preclinical studies. In particular, we show that PF-06463922 has notable and unparalleled single-agent anti-tumor activity (even at 3 mg/kg/day) in patient-derived xenograft models of *ALK*-mutated neuroblastoma for which the underlying ALK mutations were known to be associated with primary resistance to crizotinib. Moreover, treatment with PF-06463922 abrogates pALK more completely than crizotinib in xenograft tumors harboring the crizotinib-sensitive R1275Q mutation (in NB-1643 xenografts) – and promotes sustained complete regressions without subsequent tumor regrowth. With the caveat that the mouse models used here are xenografts rather than transgenic or orthotopic models, these data indicate that PF-06463922 will have much broader utility against ALK-driven neuroblastoma than any other ALK inhibitor that we have investigated – largely as a result of the substantially increased affinity for its target.

PF-06463922 is currently being investigated in a phase 1/2 clinical trial (NCT01970865) for patients with advanced NSCLC harboring ALK or ROS1 molecular alterations (16). Although most patients with ALK-translocated NSCLC derive substantial clinical benefit from crizotinib, some of these patients derive no benefit due to intrinsic resistance, and others derive initial benefit but subsequently acquire resistance through secondary *ALK* mutations and other mechanisms (22). PF-06463922 was discovered using structure-guided efforts to maintain potency across a range of resistance mutations and to optimize physicochemical properties (15). It is a potent macrocyclic ALK inhibitor with good absorption, distribution, metabolism, and excretion, as well as a low propensity for P-glycoprotein-mediated efflux and considerably improved central nervous system

penetration. PF-06463922 was also designed and optimized to penetrate the blood-brain barrier and has shown strong distribution in the central nervous system in preclinical studies (15). This is also likely to be a highly favorable attribute for use of PF-06463922 in neuroblastoma that recurs at this site (23).

Our results show that PF-06463922 inhibits various oncogenically mutated ALK variants with subnanomolar K_i values *in vitro*, and with IC_{50} values in the 10 nM range in cell viability assays. As in very recently reported preclinical studies of ALK-driven lung cancers (16), the activity of PF-06463922 did not vary significantly depending on the underlying *ALK* mutation – arguing that it will have a very broad potency in ALK-driven neuroblastomas, as well as in lung cancer. The *in vivo* responses to PF-06463922 that we report are unprecedented in ALK-driven neuroblastoma models and argue for the expedited clinical development of PF-06463922 in this disease. As is typically the case with single-agent therapies against oncogene-addicted cancers, acquired resistance to PF-06463922 is likely to arise, and future studies will need to identify the predicted mechanisms of resistance. It is important to note, however, that the major challenge for targeted therapy in ALK-driven neuroblastoma has been overcoming *de novo* resistance – and our data show that this is achieved with PF-06463922. We are therefore now poised to fast track the development of PF-06463922 to maximize clinical benefit in the subset of patients with ALK-driven neuroblastoma.

METHODS

Studies of recombinant ALK-TKD

Protein expression, purification, and analysis of kinase activity (and inhibition) was performed exactly as described by Bresler et al. (7), using unphosphorylated ALK-TKD. Kinase assays monitored incorporation of ^{32}P from γ-^{32}P ATP at 25°C. Enzyme concentration was fixed at 50 nM, and peptide and ATP concentrations were held fixed at 0.5 mM and 2 mM respectively. All data were normalized to the no inhibitor reaction after subtracting background counts from no-enzyme reaction, and were fitted to $\log_{10}$(inhibitor) vs. response nonlinear regression curve to find IC_{50} using GraphPad Prism 5.0. Triplicate experiments were run, and mean values are reported with standard deviation.

In vivo efficacy studies

The Felix and COG-N-453x PDXs and the SH-SY5Y and NB-1643 cell line-derived xenografts were implanted subcutaneously into the right flank of female CB17 SCID mice (Taconic Biosciences). PDX tumors were established in the laboratory of Dr. C. Patrick Reynolds and obtained through the Children's Oncology Group Cell Culture and Xenograft Repository. For single-agent treatment arms, mice were randomized into statistically identical cohorts at a median starting tumor volume of 200–300 mm^3 with 10 mice per group. Crizotinib (100 mg/kg QD), PF-06463922 (10 mg/kg/day, 5 mg/kg BID or 3 mg/kg/day, 1.5 mg/kg BID), and their respective vehicles were administered by oral gavage at 100 μl/10 g of body weight for a minimum of six weeks. Vehicle control mice were given 0.5% methylcellulose and 0.5% Tween-80 in water QD, and hydrochloric acid vehicle in water equimolar to the highest PF-06463922 concentration BID. Tumor size was measured two to

three times a week by digital caliper, and volume was calculated by spheroid formula (p/6) × d^3, where d represents mean diameter. According to the Institutional Animal Care and Use Committee (IUCUC) protocol, mice were removed from the study and euthanized once tumors reached $3cm^3$. This study was approved by The Children's Hospital of Philadelphia (CHOP) IACUC protocol #IAC-15-000643.

Statistical analysis of *in vivo* studies

A linear mixed effects model was used to test the difference in the rate of tumor volume change over time between different groups. The model included group, day, and group-by-day interaction as fixed effects, and included a random intercept and a random slope for each mouse. A significant group-by-day interaction would suggest that the tumor volume changes at different rates for the comparison groups. The model used vehicle group as the reference group and created separate group indicators and interaction terms for other groups. Appropriate contrast statements were created to compare the two groups other than vehicle group. If a mouse was sacrificed or removed for biological or biochemical analysis, the tumor volume was considered missing on the days afterwards. Event-free survival curves were estimated using the Kaplan-Meier method and were compared using log-rank test. Event includes death and tumor size exceeding 3 cm^3 (mouse sacrificed). Mice that were removed for biological or biochemical analysis were considered censored at the time of removal.

Cell lines and reagents

All NB cell lines (SH-SY5Y, KELLY, 415-IMDM, NBSD, Felix, NB-1643, LAN-5, NB-1, NB-EBc1, and SK-N-BE(2)C) were obtained from the CHOP cell bank in March 2013, which is routinely genotyped by short tandem repeat (STR) analysis and tested for mycoplasma. Annual genotyping (AmpFLSTR Identifiler Kit) of these lines and a single nucleotide polymorphism array analysis (Illumina H550) were performed to ensure maintenance of cell identity. The NSCLC cell line NCI-H3122 was generously provided by Jeffrey Engelman (Massachusetts General Hospital) in March 2014. Cell lines were maintained at 37°C and 5% CO_2 and cultured in RPMI 1640 media supplemented with 10% fetal bovine serum (FBS), 1% L-glutamine, 1% penicillin/streptomycin, and 0.1% gentamycin (as per provider protocol, gentamycin was not used for NCI-H3122). Felix, which was established from the same post-mortem sample as Felix-PDX, was grown in Iscove's Modified Dulbecco's Medium (IMDM) base media with 20% FBS, 1% L-glutamine, and 1% ITS (Sigma Aldrich).

In vitro pharmacologic growth inhibition

Crizotinib and PF-06463922 were provided by Pfizer, Inc. The drugs were reconstituted in 100% DMSO to a stock concentration of 10 mM and stored at −80°C. Pfizer, Inc. verified the concentrations of the stocks by mass spectrometry. Cells were plated at a density of 3,000 cells per well in triplicate in black clear-bottom tissue culture-treated 96-well plates (VWR) and treated 24 hours later with a four-log dose range of inhibitor and a DMSO control. To ensure optimal solvation, serial drug dilutions were performed in DMSO and then diluted further in starving media (0.04% FBS in RPMI or IMDM base media) before treatment. Plates were incubated for 120 h before measuring ATP levels using the CellTiter-

Glo luminescent cell viability assay (Promega) according to the manufacturer's protocol. Luminescence was measured three times per plate with a GloMax®-Multi Microplate Multimode Reader (Promega) to produce an average reading for each well. Viability assays were repeated three times per cell line. To generate IC_{50} values, the data were analyzed as follows: luminescence readings were normalized to media-only background wells and expressed as percentages of the DMSO-treated control wells. GraphPad Prism 5.0 was used to plot percent luminescence against inhibitor concentration (logarithmic scale). IC_{50} values and dose response curves were then generated using the $\log_{10}$(inhibitor) versus response nonlinear regression, defining IC_{50} as the concentration that achieves half-maximal effect where complete killing was not observed.

Focus formation assays

For focus formation assays, full-length ALK variants were subcloned into the MigR1 vector (BioPioneer, Inc.). Low-passage NIH 3T3 cells (typically <15) at ~60–70% confluence were transfected with full-length mutated ALK constructs using Lipofectamine 2000 (Invitrogen) according to the manufacturer's protocol. Cells were then allowed to recover for two days, and were transferred to 6-well plates. Each well was then topped off with medium containing DMSO as vehicle control or the appropriate concentration of inhibitor in DMSO (covering 4–5 logs). Medium (DMEM with GlutaMAX with 5% calf serum) was then changed every three days with fresh inhibitor. Focus formation typically took 10–14 days. Cells were fixed in 3.7% formaldehyde in phosphate-buffered saline (PBS) for 5 minutes and then stained with 0.05% crystal violet in distilled water for 30 minutes in order to count foci. The number of foci per well was normalized to the result seen in the DMSO control well. The half maximal inhibitory concentration (IC_{50}) was then determined from nonlinear regression analysis of a $\log_{10}$(inhibitor) versus response curve using GraphPad Prism 5.0. Each independent experiment was performed in triplicate at least, and mean values are reported with standard deviation. Western blot analysis in parallel with transfections showed similar levels of expression for the different mutants.

Western blot analysis

Between 2–3 × 10^6 cells were plated in 100 × 20 mm tissue culture dishes, allowed to attach for 24 hours, treated, and harvested on ice. Pellets were washed twice with ice cold PBS and stored at −80°C until lysis. Cells were lysed with hypotonic lysis (10 mM Tris/HCl, 10 mM NaCl, 1% Triton, 1 mM EGTA, pH 7.4) buffer with 1% protease/phosphatase inhibitor cocktail (Cell Signaling), incubated on ice for at least 15 min, and then spun in a microcentrifuge at top speed at 4°C for 5 min. Protein from the supernatant was quantified using the Bicinchoninic Acid (BCA) Assay (Thermo Scientific). Lysates (50 μg protein) were separated on NuPAGE Novex 4–12% Bis-Tris gels (Life Technologies) at 130 volts then transferred to polyvinylidene difluoride membranes (Millipore) at 4°C at 30 volts. Membranes were blocked in 5% milk or 5% bovine serum albumin fraction V, heat shock (Roche) for phospho-proteins in 1x Tris-buffered saline and Tween 20 (TBST) for 45 min at room temperature, and then incubated with primary antibodies overnight at 4°C. All primary antibodies were diluted 1:1000 except for the beta actin antibodies (1:5000). ALK pY1604, ALK pY1278, and ALK antibodies were purchased from Cell Signaling Technology, and the beta actin antibody was purchased from Santa Cruz Biotechnology. Membranes were

washed for 10 minutes three times in 1X TBST before a 45 min incubation at room temperature with the secondary antibody. Goat anti-rabbit and goat anti-mouse secondary antibodies were purchased from Cell Signaling Technology and diluted 1:5000 in 5% milk in 1X TBST. Membranes were washed again three times before developing. If necessary, membranes were stripped with a 0.1 M glycine, 0.5% Tween 20 (pH 2.5) buffer for two 15 min incubations.

Western blot analysis of xenograft tumors

At a median starting tumor volume of 200–300 mm^3, NB-1643 engrafted mice NB-1643 were randomized into groups of 3 and treated with either vehicle, crizotinib (100 mg/kg QD), or PF-06463922 (10 mg/kg/day, 5 mg/kg BID). Tumors were collected and snap frozen in liquid nitrogen after 3 days of treatment, 1 h after the final dose was administered. Tumors were homogenized in hypotonic lysis buffer with 10% protease phosphatase inhibitor cocktail in a ratio of 2000 μl lysis buffer: 0.5 g tumor. 150 μg of protein, as assessed using the BCA assay, was loaded on to gels to detect pALK.

Supplementary Material

Refer to Web version on PubMed Central for supplementary material.

Acknowledgments

The authors thank members of the Mossé lab, the Lemmon lab, Ravi Radhakrishnan, and colleagues at Pfizer for valuable discussions.

Grant Support

This work was supported in part by NIH Grant R01-CA140198 (to Y.P. Mossé), by U.S. Army Peer Reviewed Medical Research Program Grants W81XWH-10-1-0212/3 (to M.A. Lemmon and Y.P. Mossé), and by Predoctoral Fellowship 11PRE7670020 from the Great Rivers Affiliate of the American Heart Association (to J.H. Park).

References

1. Maris JM. Recent advances in neuroblastoma. N Engl J Med. 2010; 362:2202–11. [PubMed: 20558371]
2. Yu AL, Gilman AL, Ozkaynak MF, London WB, Kreissman SG, Chen HX, et al. Anti-GD2 antibody with GM-CSF, interleukin-2, and isotretinoin for neuroblastoma. N Engl J Med. 2010; 363:1324–34. [PubMed: 20879881]
3. Chen Y, Takita J, Choi Y, Kato M, Ohira M, Sanada M, et al. Oncogenic mutations of ALK kinase in neuroblastoma. Nature. 2008; 455:971–4. [PubMed: 18923524]
4. George R, Sanda T, Hanna M, Fröhling S, Luther W. Activating mutations in ALK provide a therapeutic target in neuroblastoma. Nature. 2008; 455:975–8. [PubMed: 18923525]
5. Janoueix-Lerosey I, Lequin D, Brugières L, Ribeiro A, de Pontual L, Combaret V, et al. Somatic and germline activating mutations of the ALK kinase receptor in neuroblastoma. Nature. 2008; 455:967–70. [PubMed: 18923523]
6. Mossé YP, Laudenslager M, Longo L, Cole KA, Wood A, Attiyeh EF, et al. Identification of ALK as a major familial neuroblastoma predisposition gene. Nature. 2008; 455:930–5. [PubMed: 18724359]
7. Bresler SC, Weiser DA, Huwe PJ, Park JH, Krytska K, Ryles H, et al. ALK mutations confer differential oncogenic activation and sensitivity to ALK inhibition therapy in neuroblastoma. Cancer Cell. 2014; 26:682–94. [PubMed: 25517749]

8. Schleiermacher G, Javanmardi N, Bernard V, Leroy Q, Cappo J, Rio Frio T, et al. Emergence of new ALK mutations at relapse of neuroblastoma. J Clin Oncol. 2014; 32:2727–34. [PubMed: 25071110]

9. Eleveld TF, Oldridge DA, Bernard V, Koster J, Daage LC, Diskin SJ, et al. Relapsed neuroblastomas show frequent RAS-MAPK pathway mutations. Nat Genet. 2015; 47:864–71. [PubMed: 26121087]

10. Mossé YP, Lim MS, Voss SD, Wilner K, Ruffner K, Laliberte J, et al. Safety and activity of crizotinib for paediatric patients with refractory solid tumours or anaplastic large-cell lymphoma: a Children's Oncology Group phase 1 consortium study. Lancet Oncol. 2013; 14:472–80. [PubMed: 23598171]

11. Bresler SC, Wood AC, Haglund EA, Courtright J, Belcastro LT, Plegaria JS, et al. Differential inhibitor sensitivity of anaplastic lymphoma kinase variants found in neuroblastoma. Sci Transl Med. 2011; 3:108ra14.

12. Tucker ER, Danielson LS, Innocenti P, Chesler L. Tackling crizotinib resistance: The pathway from drug discovery to the pediatric clinic. Cancer Res. 2015; 75:2770–4. [PubMed: 26122839]

13. Hallberg B, Palmer RH. Mechanistic insight into ALK receptor tyrosine kinase in human cancer biology. Nat Rev Cancer. 2013; 13:685–700. [PubMed: 24060861]

14. Fontana D, Ceccon M, Gambacorti-Passerini C, Mologni L. Activity of second-generation ALK inhibitors against crizotinib-resistant mutants in an NPM-ALK model compared to EML4-ALK. Cancer Med. 2015; 4:953–65. [PubMed: 25727400]

15. Johnson TW, Richardson PF, Bailey S, Brooun A, Burke BJ, Collins MR, et al. Discovery of (10R)-7-amino-12-fluoro-2,10,16-trimethyl-15-oxo-10,15,16,17-tetrahydro-2H-8,4-(metheno)pyrazolo[4,3-h][2,5,11]-benzoxadiazacyclotetradecine-3-carbonitrile (PF-06463922), a macrocyclic inhibitor of anaplastic lymphoma kinase (ALK) and c-ros oncogene 1 (ROS1) with preclinical brain exposure and broad-spectrum potency against ALK-resistant mutations. J Med Chem. 2014; 57:4720–44. [PubMed: 24819116]

16. Zou HY, Friboulet L, Kodack DP, Engstrom LD, Li Q, West M, et al. PF-06463922, an ALK/ROS1 inhibitor, overcomes resistance to first and second generation ALK inhibitors in preclinical models. Cancer Cell. 2015; 28:70–81. [PubMed: 26144315]

17. Cha S. Tight-binding inhibitors-I. Kinetic behavior Biochem Pharmacol. 1975; 24:2177–85. [PubMed: 1212266]

18. Mologni L, Ceccon M, Pirola A, Chiriano G, Piazza R, Scapozza L, et al. NPM/ALK mutants resistant to ASP3026 display variable sensitivity to alternative ALK inhibitors but succumb to the novel compound PF-06463922. Oncotarget. 2015; 6:5720–34. [PubMed: 25749034]

19. Cui JJ, Tran-Dubé M, Shen H, Nambu M, Kung PP, Pairish M, et al. Structure based drug design of crizotinib (PF-02341066), a potent and selective dual inhibitor of mesenchymal-epithelial transition factor (c-MET) kinase and anaplastic lymphoma kinase (ALK). J Med Chem. 2011; 54:6342–63. [PubMed: 21812414]

20. Mazot P, Cazes A, Boutterin MC, Figueiredo A, Raynal V, Combaret V, et al. The constitutive activity of the ALK mutated at positions F1174 or R1275 impairs receptor trafficking. Oncogene. 2011; 30:2017–25. [PubMed: 21242967]

21. Chand D, Yamazaki Y, Ruuth K, Schönherr C, Martinsson T, Kogner P, et al. Cell culture and Drosophila model systems define three classes of anaplastic lymphoma kinase mutations in neuroblastoma. Dis Model Mech. 2012; 6:373–82. [PubMed: 23104988]

22. Solomon B, Wilner KD, Shaw AT. Current status of targeted therapy for anaplastic lymphoma kinase-rearranged non-small cell lung cancer. Clin Pharmacol Ther. 2014; 95:15–23. [PubMed: 24091716]

23. Kramer K, Kushner B, Heller G, Cheung NK. Neuroblastoma metastatic to the central nervous system. The Memorial Sloan-Kettering Cancer Center experience and a literature review. Cancer. 2001; 91:1510–9. [PubMed: 11301399]

STATEMENT OF SIGNIFICANCE

The next generation ALK/ROS1 inhibitor PF-06463922 exerts unparalleled activity in ALK-driven neuroblastoma models with primary crizotinib resistance. Our biochemical and *in vivo* data provide the preclinical rationale for fast-tracking the development of this agent in children with relapsed/refractory ALK-mutant neuroblastoma.

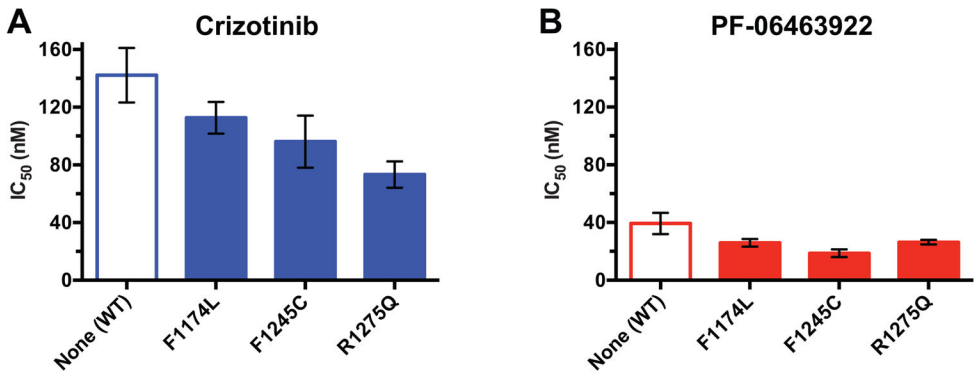

Figure 1.

PF-06463922 exhibits superior inhibitory activity against all tested ALK-TKD variants. *In vitro* inhibition profiles of purified unphosphorylated ALK-TKD protein (at 50 nM) harboring the noted mutations with **A.** crizotinib and **B.** PF-06463922. Inhibitor concentration was varied from 0 to 25,600 nM, with ATP present at 2 mM, and substrate peptide was held at 0.5 mM, as described (11). Results are plotted as mean ± SD for at least three independent experiments. As discussed in the text, the IC_{50} values obtained in this experimental format correspond to K_i values in the 6–10 nM range for crizotinib, and the 0.2 nM range for PF-06463922.

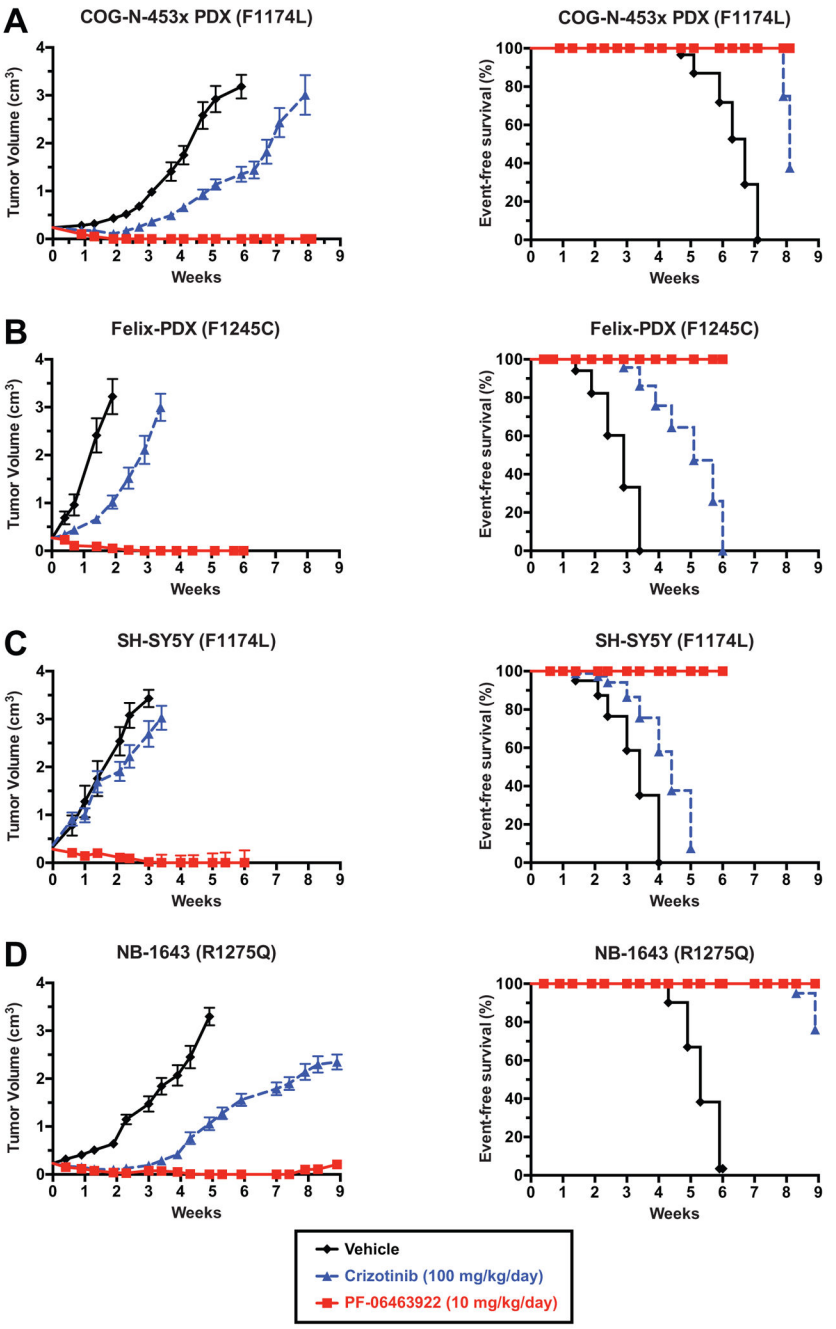

Figure 2.

PF-06463922 induces complete tumor regression in PDX and xenograft models of crizotinib-resistant and crizotinib-sensitive neuroblastoma. Subcutaneously implanted NB tumors were monitored in CB17 *scid* mice treated with 10 mg/kg/day PF-06463922 (solid red line and squares), 100 mg/kg/day crizotinib (dashed blue line and triangles), or vehicle (solid black line and diamonds). Data are shown only for the duration of treatment in each case. Study end points for survival analysis (right panels) are shown using Kaplan-Meier curves (Median ± S.E.M., n=10 for each data point). A mixed-effects linear model was used

for analysis of statistical significance of tumor growth delay. Kaplan-Meier curves for event-free survival (EFS) were compared using a log-rank test, with $p<0.05$ taken as indicating significance (see Table 1). Additional EFS data for 4–7 weeks beyond the end of treatment are plotted in Fig. S2.

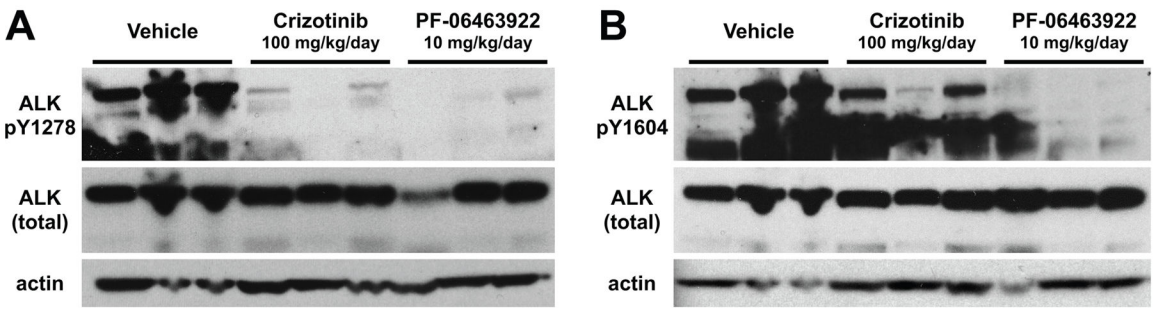

Figure 3.

PF-06463922 abrogates ALK phosphorylation more effectively than crizotinib *in vivo*. Mice harboring NB-1643 xenografts (n = 3 per arm) were treated for 3 days with vehicle, crizotinib (100 mg/kg QD), or PF-06463922 (5 mg/kg BID, 10 mg/kg/day). Tumors were harvested 1 hour after the final drug treatment, and subjected to immunoblotting as described in Methods using antibodies against pY1278 in the activation loop of the kinase (**A**) or pY1604 in the C-terminal regulatory tail (**B**), alongside control blots for total ALK and β-actin (lower panels).

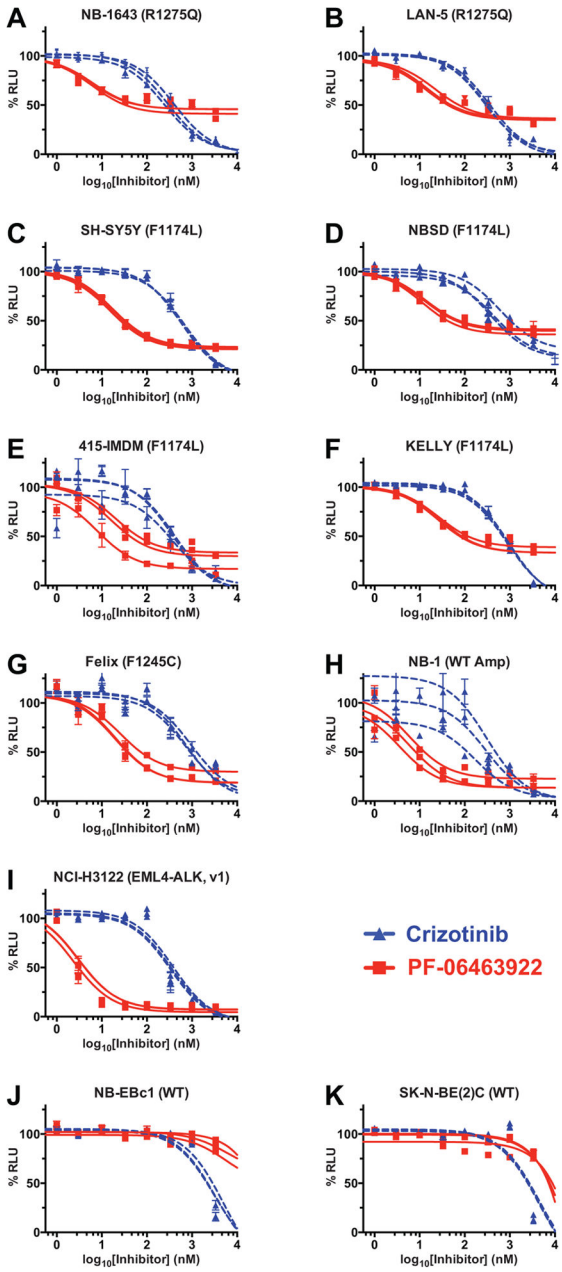

Figure 4.

PF-06463922 inhibits viability of neuroblastoma cell-lines at concentrations corresponding to clinically relevant doses (≤ 100 nM). Dose-response curves for the effects of crizotinib (dashed blue curves) and PF-06463922 (red curves) on cell viability are shown for a series of neuroblastoma cell-lines driven by R1275Q-mutated ALK (**A**, **B**); F1174L-mutated ALK (**C**–**F**), F1245C-mutated ALK (**G**), and amplified wild-type ALK (**H**). NCI-H3122 cells, driven by an ALK translocation are shown for comparison (**I**), as well as two cell-lines that are not ALK dependent (**J**, **K**). Data points are plotted as means ± SD for at least three different experiments, with blue triangles for crizotinib and red squares for PF-06463922.

The IC_{50} curves for individual experiments are also plotted, with mean IC_{50} values obtained over the three experiments listed in Table S1..

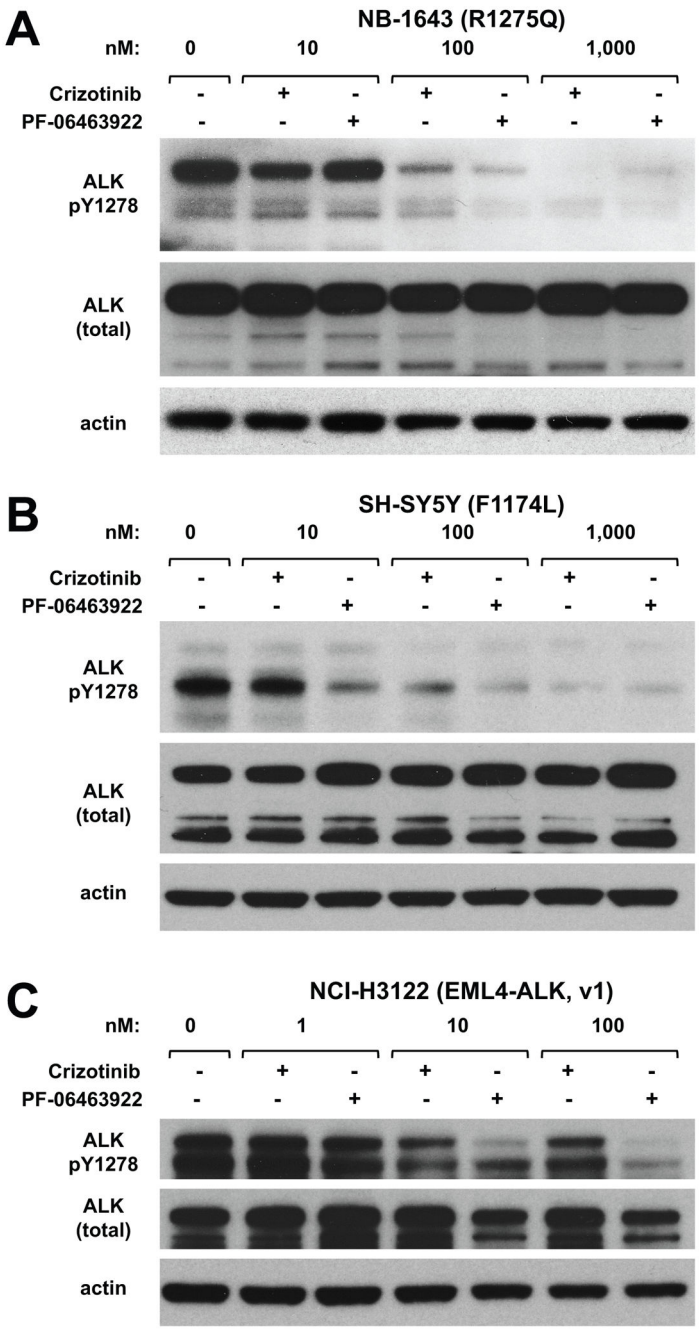

Figure 5.

PF-06463922 displays on-target activity in NB and NSCLC cells. **A.** NB-1643, **B.** SH-SY5Y, and **C.** NCI-H3122 cells were treated with increasing concentrations of crizotinib or PF-06463922. Levels of ALK autophosphorylation at Y1278 in the kinase activation loop were analyzed by Western blotting 24 hours after treatment as described in Methods.

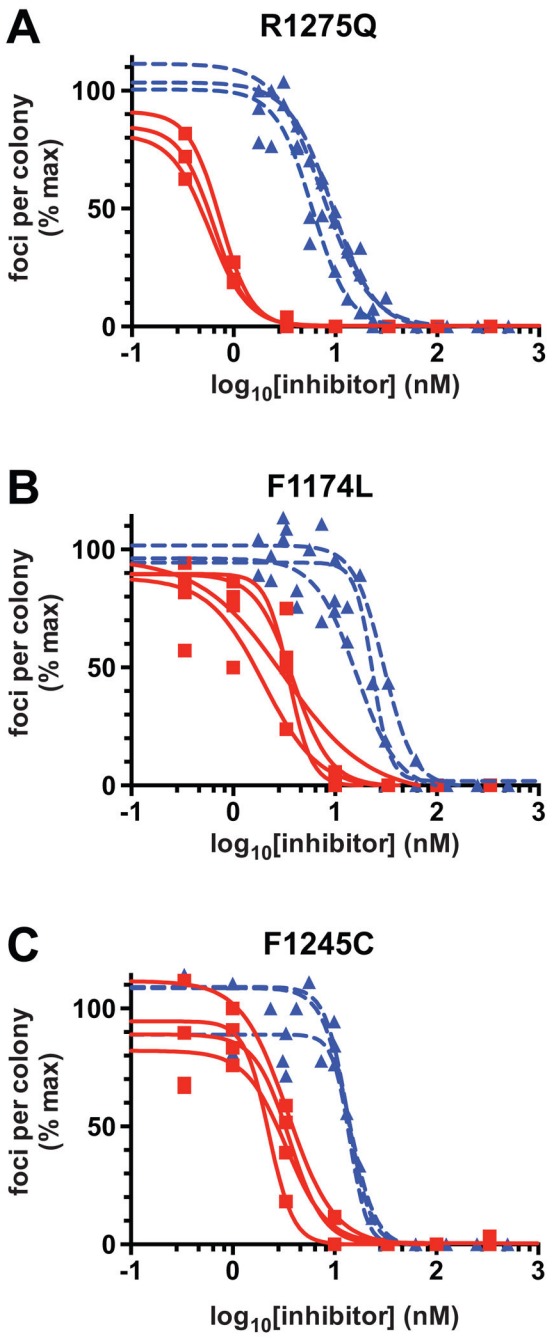

Figure 6.

PF-06463922 is more effective than crizotinib in inhibiting NIH-3T3 cell transformation by mutated ALK variants. Inhibition of NIH-3T3 cell transformation in focus-formation assays is shown for transfections with ALK harboring: (**A**) the R1275Q mutation, (**B**) the F1174L mutation, and (**C**) the F1245C mutation. The individual inhibition curves are shown for 3–4 experiments in each case for both crizotinib (blue dashed curves) and PF-06463922 (red solid curves), with data points from all experiments superimposed on the plots. Mean IC_{50}

values (± SD) for crizotinib and PF-06463922 respectively were 7.5 nM and 0.6 nM for F1275Q, 23.2 nM and 2.8 nM for F1174L, and 13.8 nM and 3.0 nM for F1245C.

Table 1

(A) Statistical analysis for *in vivo* efficacy studies in PDXs from COG-N-453x and Felix cells, and xenografts from SH-SY5Y and NB-1643 cells**. (B)** Statistical analysis for Felix-PDX and SH-SY5Y *in vivo* efficacy studies testing two doses of PF-06463922 (10 mg/kg/day and 3 mg/kg/day).

A.

PDX or xenograft (mutation)	*ALK* status	*MYCN* status	Treatment	Tumor Volume		Event-free Survival (EFS)	
				p-value vs. vehicle control	p-value vs. crizotinib	p-value vs. vehicle control	p-value vs. crizotinib
COG-N-453x	Mutated: F1174L	Amplified	Crizotinib	<0.0001		<0.0001	
			PF-06463922	<0.0001	<0.0001	<0.0001	0.0118
Felix-PDX	Mutated: F1245C	Non-amplified	Crizotinib	<0.0001		0.0008	
			PF-06463922	<0.0001	<0.0001	<0.0001	<0.0001
SH-SY5Y	Mutated: F1174L	Non-amplified	Crizotinib	0.0011		0.0502	
			PF-06463922	<0.0001	<0.0001	<0.0001	0.0003
NB-1643	Mutated: R1275Q	Amplified	Crizotinib	<0.0001		<0.0001	
			PF-06463922	<0.0001	<0.0001	<0.0001	0.1464

B.

Xenograft/PDX	*ALK* status	*MYCN* status	Treatment	Tumor Volume			Event-free Survival (EFS)		
				P-value vs. vehicle control	P-value vs. crizotinib	P-value vs. PF-06463922 (3 mg/kg/ day)	P-value vs. vehicle control	P-value vs. crizotinib	P-value vs. PF-06463922 (3 mg/kg/ day)
Felix-PDX	Mutated: F1245C	Non-amplified	Crizotinib	<0.0001			0.0008		
			PF-06463922 (3 mg/kg/day)	<0.0001	<0.0001		<0.0001	<0.0001	
			PF-06463922 (10 mg/kg/day)	<0.0001	<0.0001	0.3247	<0.0001	<0.0001	0.3428
SH-SY5Y	Mutated: F1174L	Non-amplified	Crizotinib	0.0011			0.0502		
			PF-06463922 (3 mg/kg/day)	<0.0001	<0.0001		<0.0001	0.0003	
			PF-06463922 (10 mg/kg/day)	<0.0001	<0.0001	0.6932	<0.0001	0.0003	NA